Harmonic distortion reduction in modular multilevel converters by novel mixed harmonic injection

Jayesh Kumar Motwani[1] | Luigi Piegari [2]

[1] Department of Electrical Engineering, Indian Institute of Technology (BHU), Varanasi, Uttar Pradesh, India

[2] Department of Electronics, Information and Bioengineering, Politecnico di Milano, Milan, Italy

Correspondence
Jayesh Kumar Motwani, Department of Electrical Engineering, Indian Institute of Technology (BHU), Varanasi, Uttar Pradesh, India

Email: jayeshk.motwani.eee15@iitbhu.ac.in

Abstract- This paper proposes a novel modulation scheme to reduce the harmonic content of voltages and currents caused by modular multilevel converters with embedded battery cell when employed for application in battery energy storage systems in the grid. The reduction in total harmonic distortion (THD) is obtained by injecting selected harmonics in modulating wave for phase disposition sinusoidal pulse width modulation. The main innovation is in the frequency of these injected harmonics, most of which are kept considerably higher than the carrier frequency. The injection has further been improved using closed-loop control for optimum reduction in the harmonic content of output. The simulations are performed and tested on MATLAB-SIMULINK and demonstrate a satisfactory reduction in both voltage and current THD without any counter effect.

KEYWORDS
Modular Multilevel Converter, Total Harmonic Distortion, Battery Energy Storage System, Harmonic Injection

1. INTRODUCTION

Renewable energy sources (RES) have recently gained a lot of traction for integration into the grid in recent times due to their distributed nature and environment-friendly qualities. Solar and wind energy, in particular, have acquired a significant portion of power generation capacity around the world. But, these RESs suffer from various power quality issues like grid voltage disturbances and frequency in-stabilization due to their intermittent and fluctuating power output. These issues make it difficult for the grid operators to connect these RESs to the utility grid at a large scale and can thus thwart further integration of RES in the modern power grid.

To mitigate these issues related to unreliable and intermittent nature of RESs, battery energy storage systems (BESSs) have been proposed as a viable solution. The BESSs can be used for the purpose of improving the power quality, stability, and reliability of the grid. The BESS can also provide ancillary services like load levelling, oscillation damping and power buffering[1-3]. A typical BESS fundamentally comprises of four components: an electrochemical storage, a power electronic converter, a transformer and a battery management system (BMS). While theoretically simple, the implementation of BESS into the power system has faced several challenges.

Early BESSs were based on the combination of 18-, 24-, 36-, or 48-pulse converters with complicated three-phase zigzag transformer[4-6] to lower the harmonic content injected by BESS into the grid. But these transformers are bulky, expensive and very likely to fail. In practice, almost all commercially used BESS comprise of parallel connection of two- or three-level power converters[7-10]. The output of such converters has high harmonic content. Moreover, the individual battery cells generate a much lower voltage than the power grid and hence their voltage across battery needs to be increased. This is usually achieved by forming parallel connection of multiple battery strings, each of which is itself a series connection of battery cells, thus increasing the dc voltages and power ratings. However, this further increase the complexity of the battery management system. Moreover, even if a single battery module in a battery string fails, the entire corresponding string needs to be disconnected. Such a situation either reduces the power rating drastically or forces the shutdown of the BESS for safety reasons. As a result, the probability of failure of BESS increases with the number of series-connected battery modules.

Modular multilevel converters (MMCs) stand out as one of the best alternatives for applications in BESS due to their proven reliability, elimination of the bulky and costly step-up transformer, modularity and low harmonic content[11, 12]. Current harmonics are undesirable because

of their effect the power distribution system causing additional losses in wires and cables and circuit breaker malfunctioning. Moreover, triple harmonics, being zero-sequence, increase the neutral current. Voltage harmonics, on the other hand, affect other equipment connected to the electrical system such as the erratic operation of telecommunication systems, computers, video monitors, electronic test equipment. etc., and can cause problems in insulating materials due to the high voltage derivative. But, while MMCs have lower harmonic content than other power converters currently in operation, there still is a lot of scope to further reduce the harmonic content in MMCs, thus improving the efficiency of BESSs considerably.

Passive filters have been commonly used to solve harmonic issues, but they are big, heavy and complex to be realized. To achieve high inductance values, ferromagnetic cores are usually used but, in MMCs, some dc current components could be used for balancing purposes. For this reason, the core design becomes complex to limit the size and weight of the inductor[13]. As a method to reduce the filter size while improving harmonic performance, selective harmonic elimination (SHE) has been previously discussed in the literature. Such methods rely on look up tables to derive switching angles and store them in memory for on-line working. SHE implementation further becomes even more challenging as the number of output levels increases owing to the difficulty in deriving the switching angles accurately. While SHE has the advantage of the elimination of lower order harmonics, low switching frequency and reduced switching stress[14-16], they suffer from issues of modulation ratio discretization, and controller hardware occupation[17].

Elimination of output harmonics by injection of certain signals has also recently emerged as a viable method to reduce targeted harmonics. Zero-sequence current injection has been previously proposed, achieving discontinuous modulation, which reduces switching losses and increases modulation gain[18-21]. But this results in increasing the number of submodules (SMs) since each arm requires additional SMs to avoid over-modulation and reduce SM capacitor voltage ripple. Second harmonic is injected into the arm current to optimize the current sharing among the SMs and reduce SM capacitor voltage ripple but at the expense of higher semiconductor current stresses[22, 23]. Third harmonic injection pulse width modulation (THIPWM) has been the most commonly used scheme, due to its lower harmonic content, lower SM capacitance and reduced losses[24, 25].

While much attention is paid to injection of lower harmonics, there still is a literature gap for analysis when higher order harmonics are injected with lower order harmonics. Through this research work, the authors have tried to bridge this gap by proposing a modulation technique for MMCs which considerably reduces both current and voltage total harmonic distortion (THD) by injection of both higher and lower order harmonics. The combination of higher and lower order harmonics is from hereon referred to as mixed-frequency signals. Modulating wave for phase disposition pulse width modulation (PDSPWM) is injected with higher order signals in addition to two lower order (5^{th} and 7^{th}) signals to achieve this reduction. The proposed modulation strategy works effectively for all MMCs, but is primarily designed for low module number, low frequency MMC setups. The paper is divided into seven sections; the second section discusses the basic structure of MMCs and traditional modulation strategies, the third section deals with the harmonic analysis of PDSPWM, followed by proposed modulation scheme in the fourth section. Simulation results are presented in Section five, and in section six comparison with THIPWM is presented, the paper concludes with the conclusion in section seven.

2. MMC AND TRADITIONAL MODULATION TECHNIQUES

The typical structure of MMC with embedded battery cells is shown in Figure 1. An MMC phase arm consists of cascaded connection of 'N' such submodules (SMs) or cells whose number and type can be varied according to the utility. Half-bridge SMs have been used in this paper instead of other alternative SMs like full-bridge SMs or current source SMs, because of its simple structure, high efficiency and low system cost[26]. Two such phase arms (top and bottom) are connected together, usually with inductors in middle to create a phase-leg. The submodules can be half-bridge, full-bridge or other hybrid configuration cells[27]. The submodule used in this paper comprises of a bidirectional half-bridge converter and a floating electrochemical battery cell. Each cell has two possible switching states, T_1 is on, T_2 is off ($v_0 = v_{ref}$), and T_2 is on, T_1 is off ($v_0 = 0$). The working of a single submodule is shown in Figure 2. The reference voltage v_{ref} for each cell in the submodule is given by:

$$v_{ref} = {}^{V_{DC}}/_{N} \tag{1}$$

where V_{DC} is the voltage of the virtual DC bus. On average, the number of SMs activated in a phase-leg equals N. The voltage level at the midpoint of the phase-leg is defined by the number

of SMs that are connected in the top and bottom arms of the converter. When several SMs within an arm are activated, they form a series connection of several SM voltage sources. This series connection can generate voltages greater than individual SM voltage. By regulating the total number of submodules connected in each arm of the leg, the voltage can be varied. The SMs are selected intelligently to create pseudo sinusoidal output voltage. A three-phase system consists of three phase legs. Reactors are inserted in the circuit to control the circulating currents and to limit the fault currents. MMCs with embedded battery cells further have the advantage of being able to operate at very low frequencies[28].

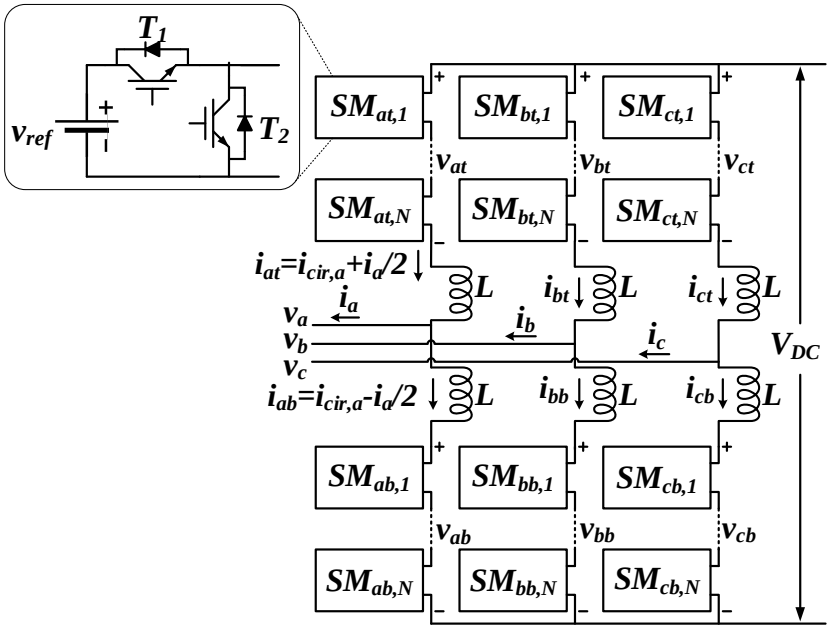

FIGURE 1. Modular Multilevel Converter

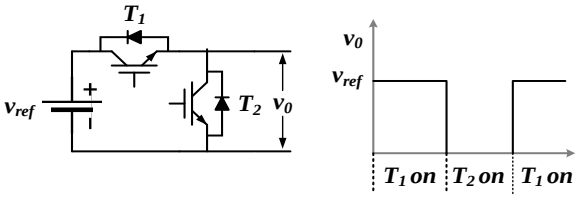

FIGURE 2. MMC Submodule

The arm currents flow through the battery cells of the active SMs and either charge or discharge the battery cells depending on their direction. The top and bottom arm currents[27] are defined as:

$$i_{kt} = i_{cir,k} + {}^{1}/_{2}\ i_k \tag{2}$$

$$i_{kb} = i_{cir,k} - {}^{1}/_{2}\ i_k \tag{3}$$

where $i_{cir,k}$ is the phase k circulating current and i_k is the phase k current. The top and bottom arm voltages for phase k are given by:

$$v_{kt} = \frac{Nv_{ref}}{2} - v_k - \frac{L}{2}\frac{di_k}{dt} - L\frac{di_{cir,k}}{dt} \tag{4}$$

$$v_{kb} = \frac{Nv_{ref}}{2} + v_k + \frac{L}{2}\frac{di_k}{dt} - L\frac{di_{cir,k}}{dt} \tag{5}$$

where v_k is the voltage of the k^{th} phase and L is the inductance of reactor. For each phase leg, differential mode voltages can be defined as:

$$v_{x,dm} = [v_{kt} - v_{kb}]/2 \tag{6}$$

For negligible L [28]:

$$v_{x,dm} \approx -v_k \tag{7}$$

As can be observed from (6) and (7), the phase leg output voltage is dependent on differential voltage only. Hence if the PWM is to be analysed, the best method would be to analyse differential voltage[29].

PDSPWM has been generally used to obtain least THD for MMCs with low number of SMs[30, 31]. To implement PDSPWM, carrier waves, each operating at frequency f_c are level displaced upon each other, and the intersection with sinusoidal waves are used to obtain switching instances for each individual submodule. In this modulation technique, the two modulating waves are displaced by 180° for the two arms in the same leg and differ by an angle of 120° among the three legs, thus generating a balanced system.

3. HARMONIC ANALYSIS OF PDSPWM

Harmonics in voltage or current waveforms are sinusoidal components of frequencies multiple of the fundamental frequency f:

$$f_h = h\,.\,f \tag{8}$$

here h is a positive integer. The periodic deviation of the voltage and current waveforms from fundamental is described in terms of the waveform distortion, often expressed using the THD. The higher the harmonic components of a quantity, the larger the distortions of this quantity, thus, larger deviations from the sinusoidal fundamental frequency. The voltage and current THDs are defined mathematically as:

$$THD_V = \frac{\sqrt{\left\{\sum_{h=2}^{\infty} {V_h}^2\right\}}}{V_1} * 100 \tag{9}$$

$$THD_I = \frac{\sqrt{\left\{\sum_{h=2}^{\infty} {I_h}^2\right\}}}{I_1} * 100 \tag{10}$$

where V_h and I_h are voltage and current rms value of the harmonic h, and V_1 and I_1 are rms value of fundamental voltage and current component.

The harmonic content of the voltage depends only on the converter whereas the harmonic content of the current depends also on the filtering action of the load and so it changes as function of the load. For this reason, harmonic content of the voltage is a better indicator of the effect of the modulation strategy on the harmonic content. Nevertheless, the harmonic content of the current, in many applications, is more important than the one for the voltage. Since the majority of the loads are inductive loads, it is preferable to move the harmonic content of the voltage in high frequency so to use the natural filtering action of the load. In order to take into account this effect and, at the same time, to obtain results that are not due to a specific load conditions, weighted THD[31] (WTHD) has been defined, giving a lower weight to high order harmonics. The WTHD is defined as:

$$WTHD = \frac{\sqrt{\left\{\sum_{h=2}^{\infty} \left\{\frac{V_h}{h}\right\}^2\right\}}}{V_1} * 100 \tag{11}$$

In this paper, for the aforementioned reasons, reference to the WTHD of the voltage will also be made.

Previous literatures[29, 33] have mathematically analysed the harmonics in differential voltage in MMC in an effort to theoretically determine the output harmonic characteristics for PDSPWM modulation. Differential voltages can be presented as:

$$v_{x,dm} = \frac{M\,V_{DC}}{2}\cos(\omega_0 t + \Theta_{x,y}) + \sum_{m=1}^{\infty}\sum_{n=-\infty}^{\infty}\frac{V_{DC}}{Nm\pi}J_{2n-1}(Nm\pi M)\cos((n-1)\pi)\cos(2m\omega_{c,pd}t + (2n-1)[\omega_o t + \Theta_{x,y}]), \quad N \text{ even} \quad (12)$$

$$v_{x,dm} = \frac{M\,V_{DC}}{2}\cos(\omega_0 t + \Theta_{x,y}) + \sum_{m=1}^{\infty}\sum_{n=-\infty}^{\infty}\frac{V_{DC}}{Nm\pi}J_{2n-1}(Nm\pi M)\cos((m+n-1)\pi)\cos(2m\omega_{c,pd}t + (2n-1)[\omega_o t + \Theta_{x,y}]), \quad N \text{ odd} \quad (13)$$

Here M is the modulation index, $J_n(\gamma)$ denotes the Bessel function of the first kind with order n and parameter γ, $\omega_{c,pd}$ is PD carrier angular frequency, ω_o is reference angular frequency, and $\Theta_{x,y}$ is phase leg reference angles. Based on (7), (12) and (13) in addition to the observations of Figure 4 and Table 1, it can be concluded that irrespective of N being odd or even, first sideband group of harmonics in the MMC operating at PDSPWM in phase voltage is centred around the frequency $2f_c$ (or$(2f_c/f)^{th}$ harmonic). These frequencies and harmonics from now on in this paper will be referred to as operating frequency and operating harmonics.

It is also worth noting that for a three phase MMC, the harmonics are of order 6p ± 1, where p is an integer. Harmonics of order 6p + 1 follow positive sequence, whereas harmonics of order 6p – 1 are of negative sequence. The injection pattern follows the pattern of phase sequence and hence the injection pattern is different for both positive and negative sequence harmonics. Interleaved PDSPWM technique is implemented for an MMC with three modules per arm operating at carrier frequency of 900 Hz. The load chosen comprises of three phase resistance and inductance of 20Ω and 30mH. The MMC is operated at unity modulation index and provides a 50Hz sinusoidal three phase output. As can be deduced from the analysis presented above and verified from Figure 3 and Table 1, the harmonics are located around 1.8kHz, satisfying the $2f_c$ condition.

The THDV, THDI and WTHD for three module per arm setup are calculated as 14.37%, 0.8% and 0.35% respectively. The operating frequency and operating harmonics are 1.8kHz and 36^{th} harmonic, respectively.

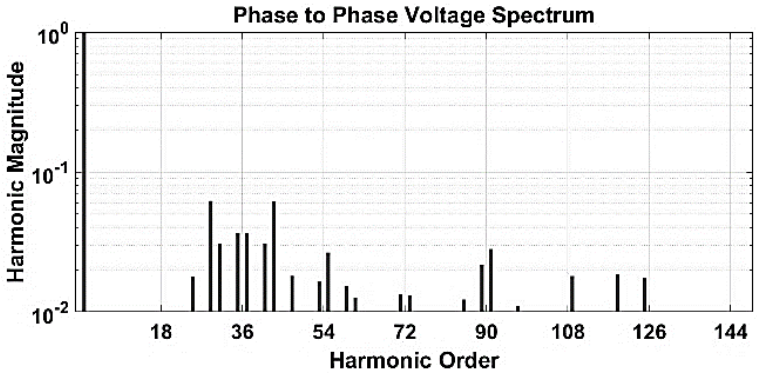

FIGURE 3. PDSPWM; N=3; f_c =900Hz; M=1

4. PROPOSED MODULATION SCHEME

The idea is to inject in the modulating signals, some harmonic components in phase opposition with the ones produced by the modulation. These injected harmonics cancel out the ones already present in the output voltage thus reducing the individual as well as the total harmonic content. Harmonic injection is a technique widely used in the technical literature. Nevertheless, usually, the order of the injected harmonic is much lower (i.e. on decade) than the switching frequency (i.e. the carrier signal frequencies). This is to avoid switching at frequencies higher than the expected one. Anyway, in MMC, the modulating signal can have high order harmonics not directly affecting the switching frequency on the basis of the implemented modulation technique. The idea of this paper is to exploit this characteristic of this converter, injecting, in the modulating signal, harmonics at frequencies higher than the switching frequency.

Since in the spectrum are present infinite harmonics, it is clear that it is necessary to choose which components have to be injected in the modulating signal. It is proved that the injection of some selected harmonics can lead to very good results in terms of THD and WTHD reduction. The pattern of sideband harmonics mentioned in previous section has been used as a reference to reduce the resulting harmonic contents. To verify the proposition, as a first step, the injection of only one harmonic is considered and then the selection and injection of multiple harmonics is analysed.

4.1 Injection of one harmonic

To demonstrate the effect of injection of higher harmonics on spectrum, a sinusoidal wave of frequency which is the next harmonic of the operating harmonic is selected. In this case, as proposed in the previous section we have considered 36th harmonic as the operating harmonic, therefore the harmonic selected to be injected is 37th harmonic. To perform harmonic injection, the amplitude and phase of 37th harmonic is fed initially from output characteristics. A sinusoidal wave of same amplitude and frequency as 37th harmonic, but in phase opposition of the selected 37th harmonic is injected in the modulating wave. A block diagram representing this idea is presented in Figure 4 and the effect of injection on harmonic spectrum is presented in Figure 5. The major harmonic content and their comparisons with the case of no harmonic injection is presented in Table 2.

As can be seen from both Figure 5 and Table 2, the targeted harmonic reduces by almost half in both voltage and current content in comparison to the case of no harmonic injection. The 37th voltage harmonic decreases to 1.95% from 3.64% whereas the total THD also comes down to 13.83% from 14.38%. But, the current THD and WTHD are increased to 0.87% and 0.38%, from 0.8% and 0.35%, respectively. This rise can be attributed to the increasing of lower order harmonics, mainly 5th and 7th harmonic.

Injection of single harmonic although results in improved THD, but the reduction in THDV is not much and in order to improve upon this, multiple harmonics are injected into the modulating wave.

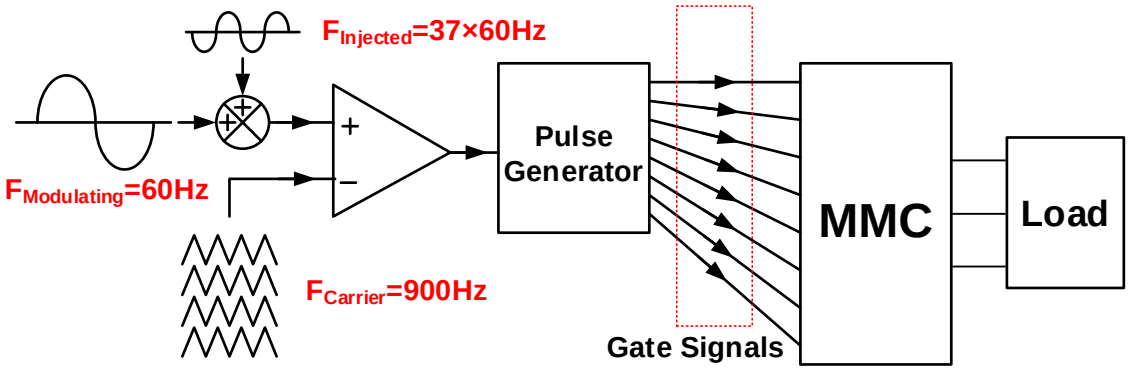

FIGURE 4. Block diagram for injection of single harmonic

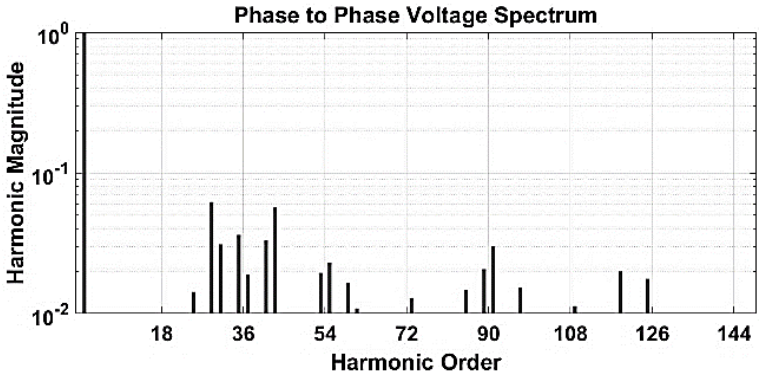

FIGURE 5. PDSPWM; N=3; f_c =900Hz; M=1; Injected harmonic: 37th

4.2 Injection of Multiple harmonics

To decrease the harmonics further, multiple higher harmonics are proposed to be injected in the modulating wave. Based on the harmonic spectrum in Figure 4, four major harmonics are proposed to be injected by authors. These are operating harmonic±1 (35th and 37th), operating harmonic-5 (31st), and operating harmonic +7 (43rd). Of these 4 harmonics, three harmonics (31st, 37th and 41st) are of positive phase sequence and one single, 35th harmonic is of negative phase sequence. After the injection of aforementioned harmonics, the THDV for three module model comes down to 11.84%, 2% reduction compared to previous case of only 37th harmonic injection. But, both THDI and WTHD increase to values 1.07% and 0.47%, from 0.87% and 0.38% respectively.

A block diagram representing the injection of multiple harmonics is presented in Figure 6. The harmonic spectrum after injection is shown is Figure 7 and the content of major harmonic with their increment or decrement compared to previous case of only 37th harmonic injection case is presented in Table 3. As can be observed, the injection of multiple harmonics causes the lower order harmonics to increase along with the neighbouring harmonics of the operating harmonic. The rise in THDI can be credited to this relocation of harmonics. Also, due to the injection, the phase and amplitude of the generated voltage harmonics changes. For this reason, in order to obtain a better cancellation of targeted harmonics, the injected harmonics need to be controlled in closed loop.

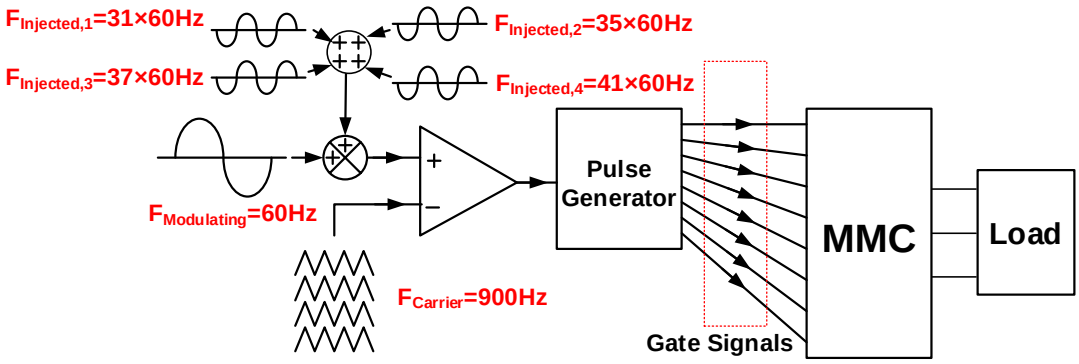

FIGURE 6. Block diagram for injection of multiple harmonics

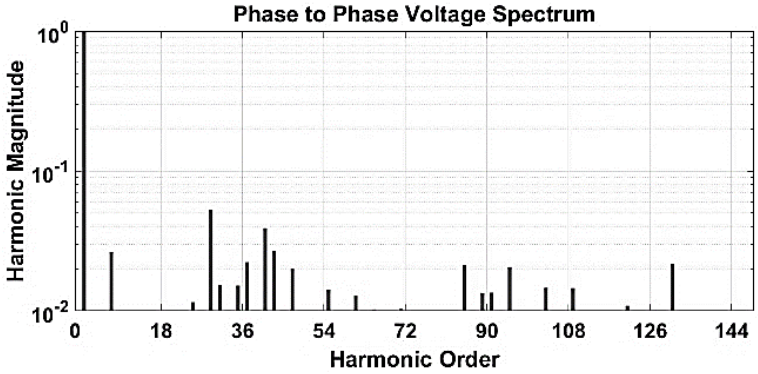

FIGURE 7. PDSPWM; N=3; f_c =900Hz; M=1; Injected harmonic: 31st, 35th, 37th and 43rd

4.3 Closed Loop Control of Harmonics

As the harmonics are injected, magnitude and phase of the targeted harmonics changes. The open loop system described above fails to consider these changes. An improvement over this is the closed loop control of the system, in which significant harmonics measured at the output are fed back in the modulating signal with same frequency and in phase opposition to the measured harmonic and with gains adjustable according to the requirement by the converter. The closed loop control block diagram is shown in Figure 8.

To elaborate upon superiority of closed loop control, the four selected harmonics of previous uncontrolled case are injected again, in closed loop control. The THDV, THDI and WTHD, all come down to 11.78%, 0.98% and 0.46%, from 11.84%, 1.07% and 0.47%, respectively. It is very evident from table that rise in THDI is due to increase in amplitude of lower order harmonics. This problem is solved in the next subsection. The harmonic spectrum after controlled injection is

plotted in the Figure 9, whereas the harmonic content of major harmonics and their increment or decrement in comparison to uncontrolled injection of these four harmonics is shown in Table 4.

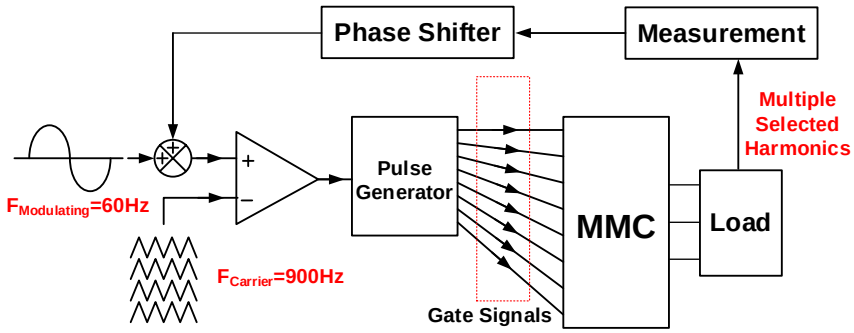

FIGURE 8. Block diagram of close loop control of harmonics

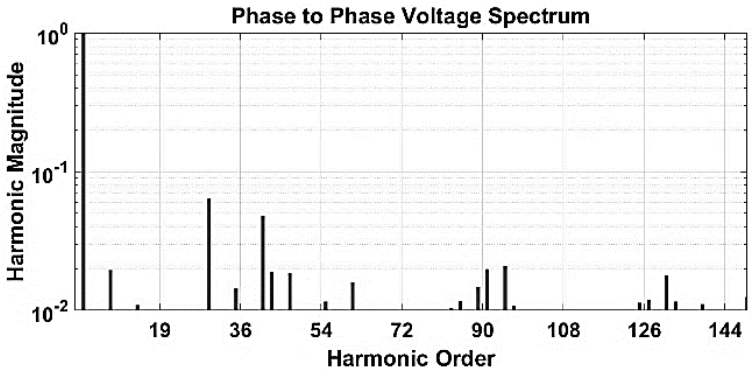

FIGURE 9. PDSPWM; N=3; f_c =900Hz; M=1; Controlled injected harmonic: 31st, 37th, 43rd and 35th

4.4 Lower Harmonic Injection

Since injection of high order harmonics presents problem of increase in lower order harmonics, lower order harmonics are also injected in the modulating signal to resolve the issue. Since 5th and 7th harmonics rise considerably by injection of higher order harmonics, these two are chosen to be fed in the modulating wave in phase opposition to the output measurements.

After injection of lower order harmonics, the THDV, THDI and WTHD come down drastically to 10.87%, 0.7% and 0.28%, respectively compared to 11.78%, 0.98% and 0.46% in the previous case of controlled injection of only higher order harmonics. The harmonic spectrum after controlled injection of both selected lower and higher order harmonics is plotted in the Figure 10, and the harmonic content of major harmonics and their increment or decrement in comparison to previous case on only higher harmonic injection is presented in Table 5.

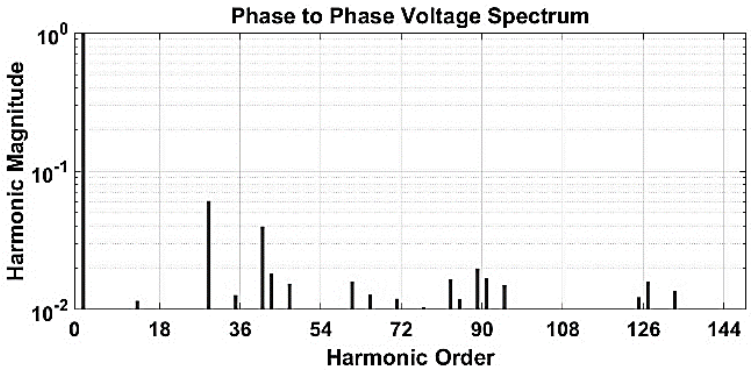

FIGURE 10. PDSPWM; N=3; f_c =900Hz; M=1; Controlled injected harmonic: 5th, 7th, 31st, 37th, 43rd and 35th

The Table 6 summarises the findings of this paper in terms of harmonic content. As can be observed, harmonic contents after injection of lower harmonics are much lower than the harmonic content without injection, thus proving efficiency of scheme by giving 25% reduction in voltage THD, 12.5% reduction in current THD and 20% reduction in WTHD. Table 7 discusses the displacement power factor, distortion power factor[34] and true power factor for the cases discussed in Table 6.

5. SIMULATION RESULTS

To verify the results presented in the paper and in order to demonstrate the applicability of the scheme in real life situation, the scheme is tested under dynamic conditions on MATLAB-SIMULINK. Figure 11 shows the variation in harmonic spectrum of modulating wave, line voltage and line current before and after the harmonic injection scheme is switched on at time t=0.2 seconds for 3 Module per arm MMC operating at 900Hz. The 3 phase RL load is set at 20Ω and 30mH. The modulating signal, as in Figure 11a and Figure 11b, has some more harmonic content after switching on the control scheme. These harmonics are injected to reduce the harmonic content. The scheme reduces the THD in the output voltage and current from 14.37% to 10.87% and 0.8% to 0.7% respectively. WTHD also comes down from 0.35% to 0.28%.

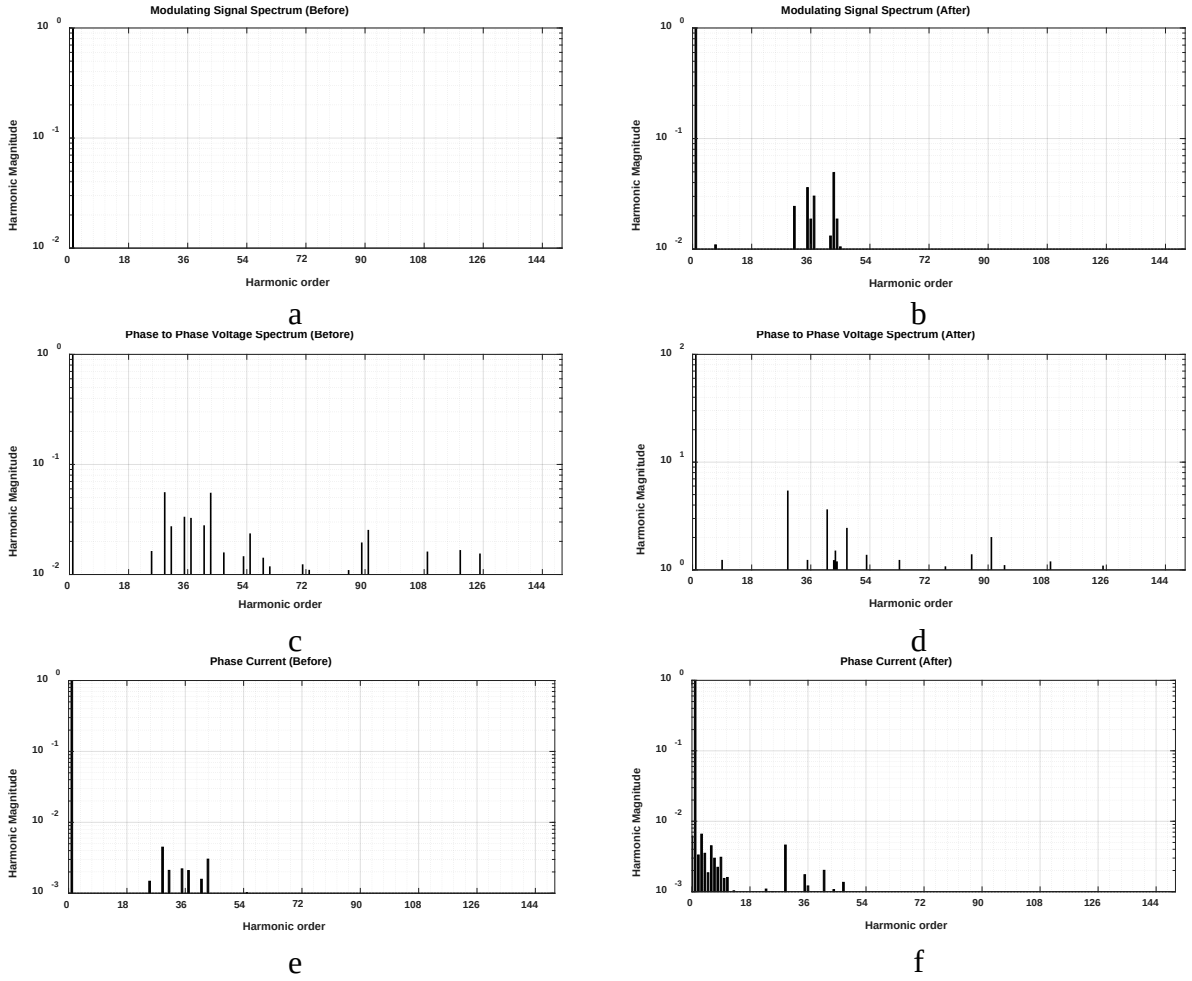

FIGURE 11. Simulations showing effect of control scheme, starting at 0.2 seconds on (a) Modulating signal (before transition), (b) Modulating signal (after transition), (c) Ph-Ph Voltage (before transition), (d) Ph-Ph Voltage (after transition), (e) Phase Current (before transition), (f) Phase Current (after transition)

The switching instances of each switch are measured in relation to time, and the average switching instances are computed by summing individual switching instances and dividing by the number of switches involved. This is simulated for both the cases of injection and non-injection of harmonics, and the results are presented in Figure 12. As is clearly visible, harmonic injection carried out to reduce THD and WTHD initially introduces some extra switching instances during the transient period, but as the system stabilises, the switching instances and hence the switching frequency in the harmonic injection case becomes lower than the case of no injection.

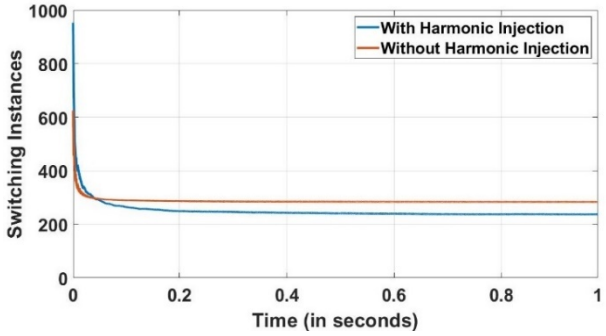

FIGURE 12. Average switching instances

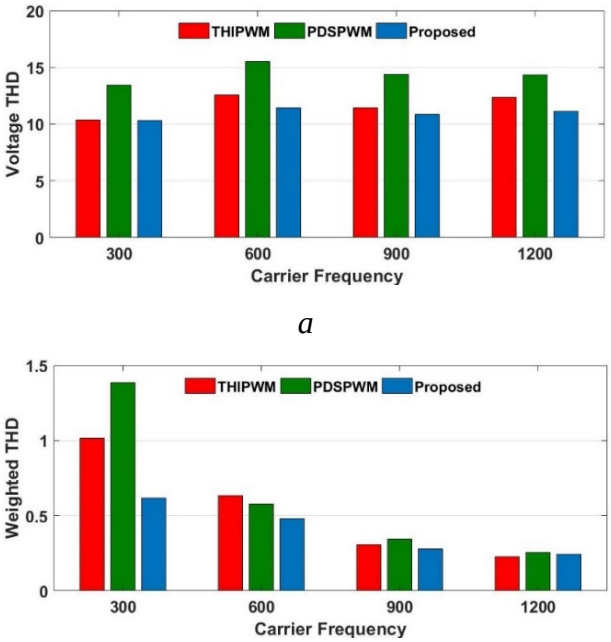

FIGURE 13. Comparison of the proposed topology on (a) Voltage THD, and (b) Weighted THD

6. COMPARISON WITH THIPWM

THIPWM has been one of the most commonly employed modulation scheme for harmonic reduction in literature[-, 25]. Figure 13a and 13b compare the performance of THIPWM with proposed modulation scheme based on voltage THD and WTHD measurements. As can be seen, the proposed modulation works significantly better at lower carrier frequencies, which is the proposed target application. Figure 14a shows the ratio of WTHD of proposed modulation over standard PDSPWM as a function of both carrier frequency and modulation. Figure 14b compares WTHD of proposed modulation with THIPWM on same parameters.

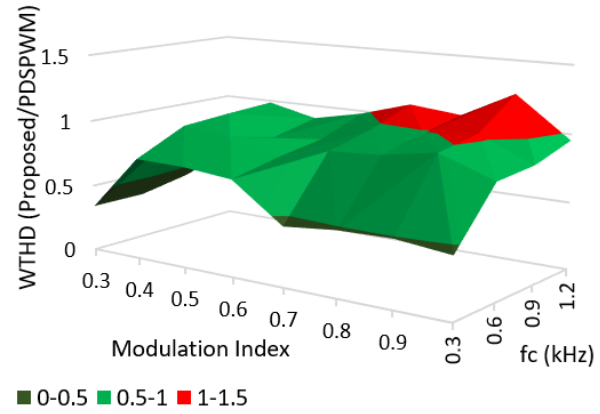

a

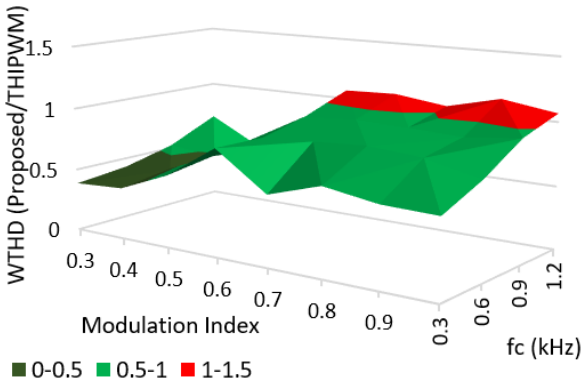

b

FIGURE 14. Ratio of WTHD in variation of Frequency and modulation, (a) Proposed vs PDSPWM, and (b) Proposed vs THIPWM

7. CONCLUSION

An innovative modulation technique to reduce THD in MMCs with embedded battery cells by injecting selected harmonics in modulating wave is proposed. The major innovation is in the frequency of these injected harmonics that is kept considerably higher than the carrier frequency. Both closed and open loop controls are discussed, and advantages and drawbacks have been discussed. Using the proposed modulation technique, voltage THD is brought down by 20-30%, current THD is brought down by around 10-15% and WTHD is brought down to 15-20%, without any counter-effect. Simulations are performed and tested on MATLAB-SIMULINK verifying

both steady state and dynamic performance of the proposed scheme. The system with control scheme is stable for both the results and is a good solution to be used in high precision, low frequency, low module count modular multilevel converters. The proposed modulation is compared to PDSPWM and THIPWM to demonstrate the improvements that controlled harmonic injection provides.

8. REFERENCES

1. Byrne, R. H., Nguyen, T. A., Copp, D. A., Chalamala, B. R., & Gyuk, I. (2018). Energy management and optimization methods for grid energy storage systems. IEEE Access, 6, pp.13231-13260
2. Hu, C. Zou, C. Zhang, & Y. Li, (2017). Technological developments in batteries: a survey of principal roles, types, and management needs. IEEE Power and Energy Magazine, 15(5), pp.20-31
3. Lai, J., Song, Y., & Du, X. (2018). Hierarchical Coordinated Control of Flywheel Energy Storage Matrix Systems for Wind Farms. IEEE/ASME Transactions on Mechatronics, 23(1), pp.48-56,
4. Walker, L. H. (1990). 10-MW GTO converter for battery peaking service. IEEE Trans. Ind. Appl., vol. 26, no. 1, pp. 63–72.
5. Saupe, R. (1988) The power conditioning system for the +/-8,5/17 MWenergy storage plant of BEWAG. Conf. Proc. Third International Conference on Power Electronics and Variable-Speed Drives, pp. 218–220.
6. Ota, J. I. Y., Sato T., & Akagi H. (2016). Enhancement of performance availability and flexibility of a battery energy storage system based on a modular multilevel cascaded converter (MMCC-SSBC). IEEE Trans. Power Electron. vol. 31 no. 4 pp. 2791-2799
7. Devries, T., Mcdowall, J., Umbricht, N., & Linhofer, G. (2004). Cold storage. ABB Review, no. 1, pp. 38–43.
8. Wade, N., Taylor, P., Lang, P., & Svensson, J. (2009). Energy storage for power flow management and voltage control on an 11-kV UK distribution network. Conf. Proc. 20th International Conference and Exhibition on Electricity Distribution - Part 1, 2009. CIRED 2009.

9. Li, H., Iijima, Y., & Kawakami, N. (2013). Development of power conditioning system (PCS) for battery energy storage systems. Proc. Conf. 2013 IEEE ECCE Asia Downunder (ECCE Asia), pp. 1295– 1299
10. Kawakami, N., Iijima, Y., Li, H., & Ota, S. (2014). High efficiency power converters for battery energy storage systems. The 2014 International Power Electronics Conference (IPEC-Hiroshima 2014 - ECCE-ASIA), pp. 2095–2099
11. Judge, P. D., & Green, T. C. (2019). Modular Multilevel Converter with Partially Rated Integrated Energy Storage Suitable For Frequency Support and Ancillary Service Provision. IEEE Trans. Power Electron. vol. 34 no. 1 pp. 208-219
12. Shi, Y., & Li, H. (2018). Isolated modular multilevel DC–DC converter with DC fault current control capability based on current-fed dual active bridge for MVDC application. *IEEE Trans. Power Electron.*, vol. 33, no. 3, pp. 2145-2161
13. Beres, R. N., Wang, X., Liserre, M., Blaabjerg, F., & Bak, C. L. (2016). A review of passive power filters for three-phase grid-connected voltage source converters. IEEE J. Emerg. Sel. Topics Power Electron., vol. 4, no. 1, pp. 54–69
14. Li, R., & Fletcher, J. E. (2017). A novel MMC control scheme to increase the DC voltage in HVDC transmission systems. Electric Power Systems Research, 143, pp. 544–553.
15. Konstantinou, G., Ciobotaru, M., & Agelidis, V. (2013). Selective harmonic elimination pulse-width modulation of modular multilevel converters. IET Power Electron., 6, pp. 96–107.
16. Konstantinou, G., Ciobotaru, M., & Agelidis, V. (2011). Operation of a modular multilevel converter with selective harmonic elimination PWM. Power Electronics and ECCE Asia (ICPE & ECCE), 2011 IEEE 8th International Conference, pp. 999–1004.
17. Du, Sixing & Liu, Jinjun & Liu, Teng. (2015). A PDPWM Based DC Capacitor Voltage Control Method for Modular Multilevel Converters. Journal of Power Electronics. 15. 660-669.
18. Picas, R., Ceballos, S., Pou, J., Zaragoza, J., Konstantinou, G., & Agelidis, V.G. (2013). Improving capacitor voltage ripples and power losses of modular multilevel converters through discontinuous modulation. Industrial Electronics Society, IECON 2013-39th Annual Conference of the IEEE, 6233–6238.

19. Picas, R., Ceballos, S., Pou, J., Zaragoza, J., Konstantinou, & G., Agelidis, V.G. (2015). Closed-loop discontinuous modulation technique for capacitor voltage ripples and switching losses reduction in modular multilevel converters. IEEE Trans. Power Electron. 30 4714–4725.
20. Song, Q., Liu, W., Li, X., Rao, H., Xu, S., & Li, L. (2013). A steady-state analysis method for a modular multilevel converter. IEEE Trans. Power Electron., vol. 28, no. 8, pp. 3702–3713.
21. Li, X., Song, Q., Liu, W., Xu, S., Zhu, Z., & Li, X. (2016). Performance analysis and optimization of circulating current control for modular multilevel converter. IEEE Trans. Ind. Electron., vol. 63, no. 2, pp. 716–727
22. Rasic, Krebs U., Leu, H., & Herold, G.: 'Optimization of the modular multilevel converters performance using the second harmonic of the module current', Power Electronics and Applications, 2009. EPE '09. 13th European Conference on (2009) 1–10
23. Wu. D., Peng, L. (2016). Analysis and suppressing method for the output voltage harmonics of modular multilevel converter. IEEE Trans. Power Electron., vol. 31, no. 7, pp. 4755–4765
24. Islam, M.R., Youguang, G., & Jianguo, Z. (2014). A high-frequency link multilevel cascaded medium-voltage converter for direct grid integration of renewable energy systems. IEEE Trans. Power. Electron., 29, (8), pp. 4167–4182
25. Li, R., Fletcher, J. E., & Williams, B. W. (2016). Influence of third harmonic injection on modular multilevel converter-based high-voltage direct current transmission systems. IET Gener., Transm. Distrib., vol. 10, no. 11, pp. 2764–2770.
26. Wang, Y., Aksoz, A., Geury, T., Ozturk, S.B., Kivanc, O.C., Hegazy, O. (2020) A Review of Modular Multilevel Converters for Stationary Applications. Appl. Sci., vol. 10, no. 21, 7719.
27. Du, S., Dekka, A., Wu, B., Zargari, N. (2018). Modular Multilevel Converters Analysis, Control, and Applications (IEEE Press Series on Power Engineering). Wiley-IEEE Press
28. D'Arco, S., Quraan, M., Tricoli, P., & Piegari, L., (2016). Low frequency operation of Modular Multilevel Converters with embedded battery cells for traction drives. International Symp. Power Electron., Elect. Drives, Automat. Motion, pp. 1375–1382

29. McGrath, B. P., Teixeira, C. A, & Holmes, D. G. (2017). Optimized Phase Disposition (PD) Modulation of a Modular Multilevel Converter. *IEEE Transactions on Industry Applications*, vol. 53, no. 5, pp. 4624–4633
30. Moranchel, M., Huerta, F., Sanz, I., Bueno, E., & Rodríguez, F. (2016). A Comparison of Modulation Techniques for Modular Multilevel Converters. Energies, 9(12), 1091.
31. Darus, R., Konstantinou, G., Pou, J., Ceballos, S., & Agelidis, V. G.(2014). Comparison of phase-shifted and level-shifted PWM in the modular multilevel converter. International Power Electronics Conference (IPEC-Hiroshima 2014 - ECCE ASIA).
32. Lipo, T. (2000). An improved weighted total harmonic distortion index for induction motor drives. Proc. Int. Conf. Optim. Elect. Electron. Equip., vol. 2, pp. 311–322
33. McGrath, B. P., Holmes, D. G. (2002). Multicarrier PWM strategies for multilevel inverters. *IEEE Trans. Ind. Electron.*, vol. 49, no. 4, pp. 858-867
34. Cividino, L. (1992). Power factor, harmonic distortion; causes, effects and considerations. Fourteenth International Telecommunications Energy Conference - INTELEC '92, Washington, DC, USA, 1992, pp. 506-513

TABLE 1. Major harmonics for interleaved PDSPWM; N=3; f_c =900Hz; M=1

Harmonic order	Voltage [%]	Current [%]
5	0.03	0.01
7	0.05	0.02
29	6.19	0.50
31	3.11	0.23
35	3.65	0.24
37	3.64	0.23
41	3.07	0.18
43	6.19	0.34

TABLE 2. Harmonic content for interleaved PDSPWM; N=3; f_c =900Hz; M=1; Injected harmonic: 37^{th}

Harmonic order	Voltage [%] (% change)	Current [%] (% change)
5	0.52 (+1633%)	0.22 (+2100%)
7	0.97 (+1840%)	0.31 (+1450%)
29	6.24 (+0.8%)	0.50 (+0%)
31	3.08 (-0.64%)	0.23 (+0%)
35	3.64 (-0.27%)	0.24 (+0%)
37	1.95 (-46%)	0.12 (-48%)
41	3.31 (+7%)	0.19 (+5%)
43	5.72 (-7%)	0.31 (-9%)

TABLE 3. Major harmonics for interleaved PDSPWM; N=3; f_c =900Hz; M=1; Injected harmonic: 31st, 35th, 37th, and 43rd

Harmonic order	Voltage [%] (% change)	Current [%] (% change)
5	0.26 (-50%)	0.11 (+50%)
7	2.66 (+174%)	0.85 (+174%)
29	5.21 (-17%)	0.42 (-16%)
31	1.65 (-46%)	0.12 (-48%)
35	1.41 (-61%)	0.09 (-63%)
37	2.32 (+18%)	0.15 (+25%)
41	3.92 (+18%)	0.22 (+16%)
43	2.84 (-50%)	0.16 (-48%)

TABLE 4. Harmonic content for PDSPWM; N=3; f_c =900Hz; M=1; Controlled injected harmonic: 31st, 37th, 43rd and 35th

Harmonic order	Voltage [%] (% change)	Current [%] (% change)
5	0.75 (+188%)	0.31 (+182%)
7	1.89 (-29%)	0.62 (-27%)
29	6.19 (+18%)	0.52 (+23%)
31	1.12 (-32%)	0.08 (-33%)
35	1.39 (-1%)	0.10 (+11%)
37	0.91 (-61%)	0.06 (-60%)
41	4.49 (+14%)	0.26 (+18%)
43	2.55 (-10%)	0.14 (-13%)

TABLE 5. Harmonic content for PDSPWM; N=3; f_c =900Hz; M=1; Controlled injected harmonic: 5^{th}, 7^{th}, 31^{st}, 37^{th}, 43^{rd} and 35^{th}

Harmonic order	Voltage [%] (% change)	Current [%] (% change)
5	0.32 (-58%)	0.13 (-58%)
7	0.55 (-71%)	0.18 (-71%)
29	5.81 (-6%)	0.47 (-10%)
31	0.73 (-35%)	0.05 (-37%)
35	0.77 (-44%)	0.05 (-50%)
37	0.58 (-36%)	0.04 (-33%)
41	3.43 (-23%)	0.20 (-23%)
43	2.30 (-10%)	0.13 (-7%)

TABLE 6. Summary

Harmonics Injected	Method of injection	VTHD [%] (% change)	ITHD [%] (% change)	WTHD [%] (% change)
None	-	14.37%	0.8%	0.35%
37	U*	13.83% (-4%)	0.87% (+8%)	0.38% (+9%)
31, 35, 37 and 43	U*	11.84% (-17%)	1.07% (+33%)	0.47% (+34%)
31, 35, 37 and 43	C*	11.78% (-18%)	0.98% (+22%)	0.46% (+31%)
5, 7, 31, 35, 37 and 43	C*	10.87% (-24%)	0.7% (-13%)	0.28% (-20%)

U*: Uncontrolled Injection, C*: Controlled Injection

TABLE 7. Power Factor Summary

Harmonics Injected	Method of injection	ITHD [%] (% change)	Displacement Power Factor	Distortion Power Factor	True Power Factor
None	-	0.8%	0.9046	0.99997	0.90457
37	U*	0.87% (+8%)	0.9046	0.99996	0.90456
31, 35, 37 and 43	U*	1.07% (+33%)	0.9046	0.99994	0.90454
31, 35, 37 and 43	C*	0.98% (+22%)	0.9046	0.99995	0.90455
5, 7, 31, 35, 37 and 43	C*	0.7% (-13%)	0.9046	0.999975	0.90458

U*: Uncontrolled Injection, C*: Controlled Injection